First-principles study on the conventional superconductivity of N-doped *fcc*-LuH₃ Ⓕ

View Online   Export Citation   CrossMark

Zihao Huo,[1] ⁣🄳 Defang Duan,[1,a] ⁣🄳 Tiancheng Ma,[1] Zihan Zhang,[1] Qiwen Jiang,[1] Decheng An,[1] Hao Song,[2] Fubo Tian,[1] ⁣🄳 and Tian Cui[1,2a]

AFFILIATIONS

[1] State Key Laboratory of Superhard Materials, College of Physics, Jilin University, Changchun 130012, China
[2] Institute of High Pressure Physics, School of Physical Science and Technology, Ningbo University, Ningbo 315211, China

[a] Authors to whom correspondence should be addressed: duandf@jlu.edu.cn and cuitian@nbu.edu.cn

ABSTRACT

Recently, room-temperature superconductivity has been reported in a nitrogen-doped lutetium hydride at near-ambient pressure [Dasenbrock-Gammon *et al.*, Nature **615**, 244 (2023)]. The superconducting properties might arise from $Fm\overline{3}m$-LuH$_{3-\delta}$N$_\varepsilon$. Here, we systematically study the phase diagram of Lu–N–H at 1 GPa using first-principles calculations, and we do not find any thermodynamically stable ternary compounds. In addition, we calculate the dynamic stability and superconducting properties of N-doped $Fm\overline{3}m$-LuH$_3$ using the virtual crystal approximation (VCA) and the supercell method. The $R3m$-Lu$_2$H$_5$N predicted using the supercell method could be dynamically stable at 50 GPa, with a T_c of 27 K. According to the VCA method, the highest T_c is 22 K, obtained with 1% N-doping at 30 GPa. Moreover, the doping of nitrogen atoms into $Fm\overline{3}m$-LuH$_3$ slightly enhances T_c, but raises the dynamically stable pressure. Our theoretical results show that the T_c values of N-doped LuH$_3$ estimated using the Allen–Dynes-modified McMillan equation are much lower than room temperature.

I. INTRODUCTION

Hydrides have received much attention because of their excellent superconductivities under pressure.[1–4] In 2014, H$_3$S was predicted to be a high-temperature superconductor with a T_c of 191–204 K,[5] which was confirmed by the experimentally measured T_c of 203 K at 155 GPa.[6,7] Following this success, several superhydrides with high T_c values above 200 K, such as LaH$_{10}$ (260 K, 170 GPa), YH$_6$ (224 K, 166 GPa), YH$_9$ (260 K, 201 GPa), and CaH$_6$ (215 K, 172 GPa), were predicted and synthesized.[8–18] Recently, Song *et al.*[19] comprehensively studied the Lu–H system and predicted that $Im\overline{3}m$-LuH$_6$ should have a T_c of 273 K at 100 GPa. Extensive experimental research has been conducted on the superconducting properties of lutetium hydrides under pressure. $Fm\overline{3}m$-LuH$_3$ has been successfully synthesized and found to have a T_c of 12 K at 122 GPa.[20] Moreover, $Pm\overline{3}n$-Lu$_4$H$_{23}$ has been obtained, with a T_c of 71 K at 218 GPa.[21] In particular, a very recent experimental study has reported superconductivity in the Lu–N–H

system at near-ambient pressure (~1 GPa), with the highest T_c to date of 294 K,[22] thus achieving room-temperature superconductivity near ambient pressure. The authors of this study attributed the room-temperature superconductivity in the Lu–N–H system to $Fm\overline{3}m$-LuH$_{3-\delta}$N$_\varepsilon$, which can be regarded as $Fm\overline{3}m$-LuH$_3$ doped with nitrogen atoms.

This report could represent a landmark event for the scientific community, but many open questions surrounding this important discovery remain unanswered, for example, the exact stoichiometry and the positions of the hydrogen and nitrogen atoms. A subsequent experimental observation indicates that the pressure-induced color change of LuH$_2$ is similar to that of N-doped lutetium hydride.[23] In addition, a similar compound (LuH$_{2\pm x}$N$_y$) has been synthesized, but no evidence for superconductivity at pressures ranging from 1 to 6 GPa has been found.[24] Density functional theory (DFT) calculations have been used to investigate the optical properties of lutetium hydrides[25] and the phase diagram of the Lu–N–H system at 0, 5, and 10 GPa,[26] but no thermodynamically stable

ternary compounds have been found. Therefore, an investigation of the superconducting properties of N-doped lutetium hydrides is necessary.

In the work described in this paper, we performed a comprehensive first-principles study on the Lu–N–H system at 1 GPa. No thermodynamically stable Lu–N–H ternary compounds were found using the structure search method. We then analyzed the dynamic stability and superconducting properties of N-doped $Fm\overline{3}m$-LuH$_3$ using the virtual crystal approximation (VCA) and the supercell method. Using the Allen–Dynes-modified McMillan (A-D-M) equation, we found that the estimated highest T_c of N-doped LuH$_3$ did not exceed 30 K, which is much lower than room temperature. In addition, we found that the doping of nitrogen atoms may slightly enhance T_c but also increase the dynamically stable pressure of LuH$_3$.

II. COMPUTATIONAL DETAILS

At 1 GPa, we performed a variable-composition crystal structure search in the Lu–N–H system with ~10 000 structures using the *Ab Initio* Random Structure Searching (AIRSS)[27] code. We then re-optimized the structures using the *ab initio* calculation from the Cambridge Serial Total Energy Package (CASTEP).[28] An on-the-fly ultrasoft pseudopotential with valence electrons $1s^1$ for H, $2s^2 2p^3$ for N, and $4f^{14} 5s^2 5p^6 5d^1 6s^1$ for Lu was used, with a kinetic cutoff energy of 800 eV. The Brillouin zone was sampled using a k-point mesh of $2\pi \times 0.03$ Å^{-1} to make the enthalpy calculations converge well to less than 1 meV/atom. Structural relaxations were performed using projector-augmented wave (PAW)[29,30] potentials, as implemented in the Vienna *Ab Initio* Simulation Package (VASP),[31] with a cutoff energy of 600 eV. The exchange-correlation functional was described using the Perdew–Burke–Ernzerhof generalized gradient approximation.[32]

We then prepared a conventional cell of $Fm\overline{3}m$-LuH$_3$, including four formula units (f.u.). The calculations were performed for a range of pseudostoichiometric Lu$_4$H$_m$N$_{12-m}$, including Lu$_4$H$_{11}$N, Lu$_2$H$_5$N, Lu$_4$H$_9$N$_3$, and LuH$_2$N, which correspond to nitrogen-to-hydrogen atomic ratios of 0.09, 0.2, 0.33, and 0.5, respectively. Next, we calculated the formation enthalpies and superconducting properties of these structures at 1, 10, and 50 GPa. The formation enthalpy of Lu$_4$H$_m$N$_{12-m}$ was calculated using the following equation:

$$H^f = H(\text{Lu}_4\text{H}_m\text{N}_{12-m}) - 4H(\text{LuH}_3) - mH(\text{N}) + mH(\text{H}). \quad (1)$$

We investigated the pressure dependence of the superconductivity of $Fm\overline{3}m$-LuH$_3$ at 0.5%–2% doping with N using the VCA at pressures below 100 GPa. The VCA was performed by generating a virtual pseudopotential V_{VCA} of H$_{1-x}$N$_x$, where $V_{\text{VCA}} = (1 - x) V_{\text{H}} + xV_{\text{N}}$. Furthermore, we calculated the equation of state for LuH$_{2.97}$N$_{0.03}$, which is close to the elemental analysis data from previous experiments,[22] using DFT and DFT + U (with $U = 5.5$ eV, which has been used for metal mononitrides[22]). The result is shown in Fig. S1 (supplementary material). The DFT result without the Hubbard U effect fits better with the experimental data. Therefore, the DFT level calculation for N-doped LuH$_3$ is acceptable.

Electronic structures, phonon spectra, and electron–phonon coupling (EPC) were calculated using the QUANTUM ESPRESSO (QE)[33] package. The PAW pseudopotentials with valence electrons $1s^1$ for H, $2s^2 2p^3$ for N, and $5s^2 5p^6 5d^1 6s^2$ for Lu were used in the QE package. The self-consistent electron density was evaluated using a k-mesh of $20 \times 20 \times 20$. The phonon spectra and EPC were calculated using a q-mesh of $5 \times 5 \times 5$. The conventional superconducting transition temperature was estimated using the A-D-M equation[34]
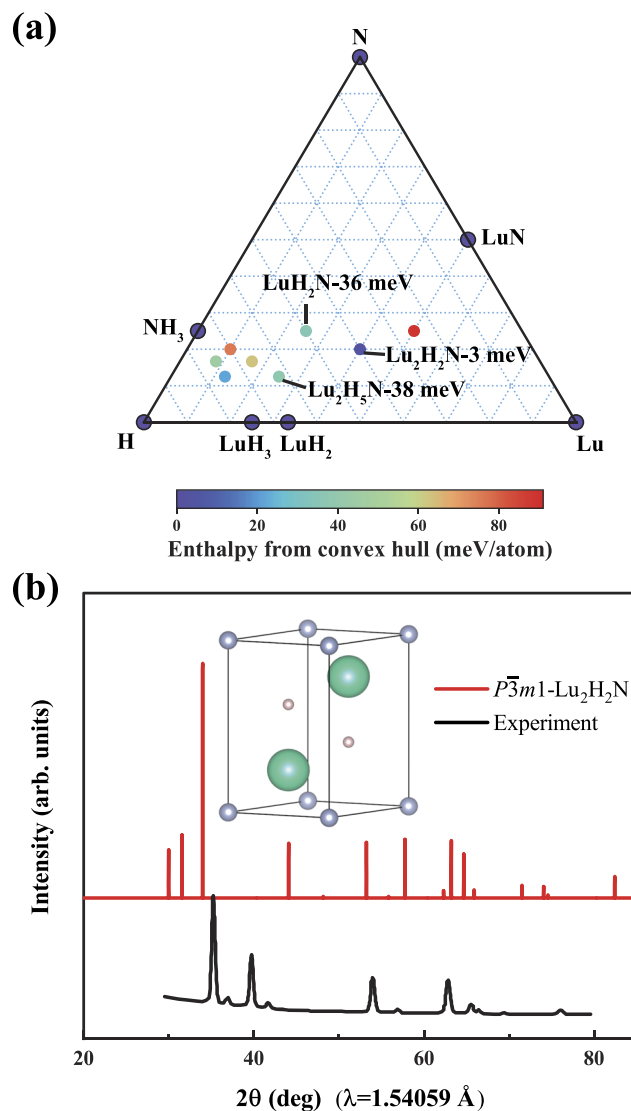
(a)

(b)

FIG. 1. (a) Ternary phase diagram (convex hull) of the Lu–N–H system at 1 GPa. The values of the enthalpy from the convex hull are shown next to the colored circles. The circles with black solid boundaries denote the stable phases. (b) Comparison of the XRD pattern from reported experimental data[22] (lower black curve) and the pattern calculated for $P\overline{3}m1$-Lu$_2$H$_2$N at ambient pressure (upper red curve). The inset shows the crystal structure of $P\overline{3}m1$-Lu$_2$H$_2$N, with green, gray, and pink spheres depicting Lu, N, and H atoms, respectively.
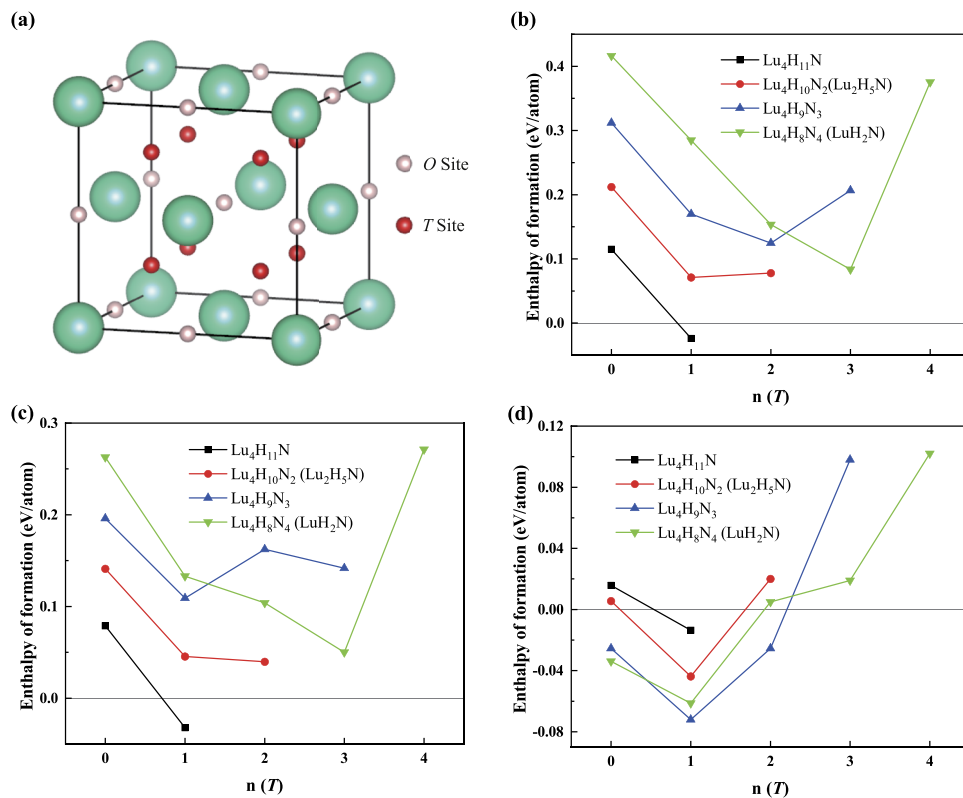
FIG. 2. (a) Crystal structure of $Fm\bar{3}m$-LuH_3 with different types of H occupancy sites. Green spheres depict Lu atoms; pink and red spheres depict H occupancy of O and T sites, respectively. (b)–(d) Calculated enthalpy of formation of $Lu_4H_mN_{12-m}$ as a function of T-site occupancy at 1, 10, and 50 GPa, respectively. $n(T)$ is the number of nitrogen atoms in each stoichiometry occupying T sites.
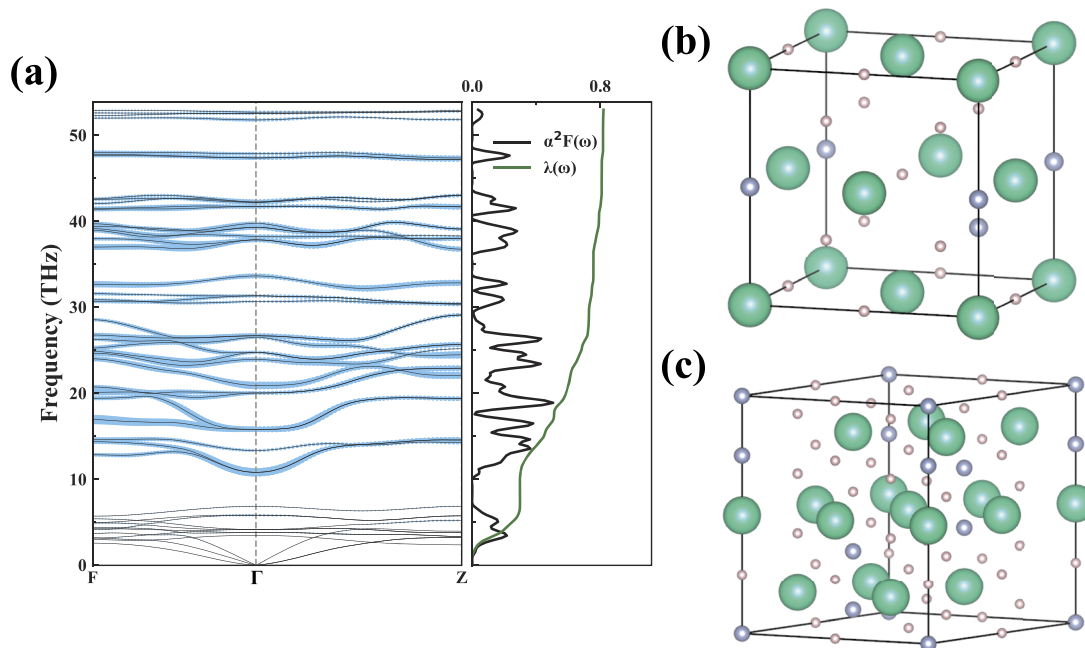

FIG. 3. (a) Phonon spectra, Eliashberg phonon spectral function $\alpha^2F(\omega)$, and electron–phonon integral λ for $R3m$-Lu_2H_5N at 50 GPa. The magnitudes of the phonon linewidths are represented by the sizes of the blue circles. (b) and (c) Crystal structures of $R3m$-Lu_2H_5N in the framework of $Fm\bar{3}m$-LuH_3 and the conventional cell, respectively. Green, gray, and pink spheres depict Lu, N, and H atoms, respectively.
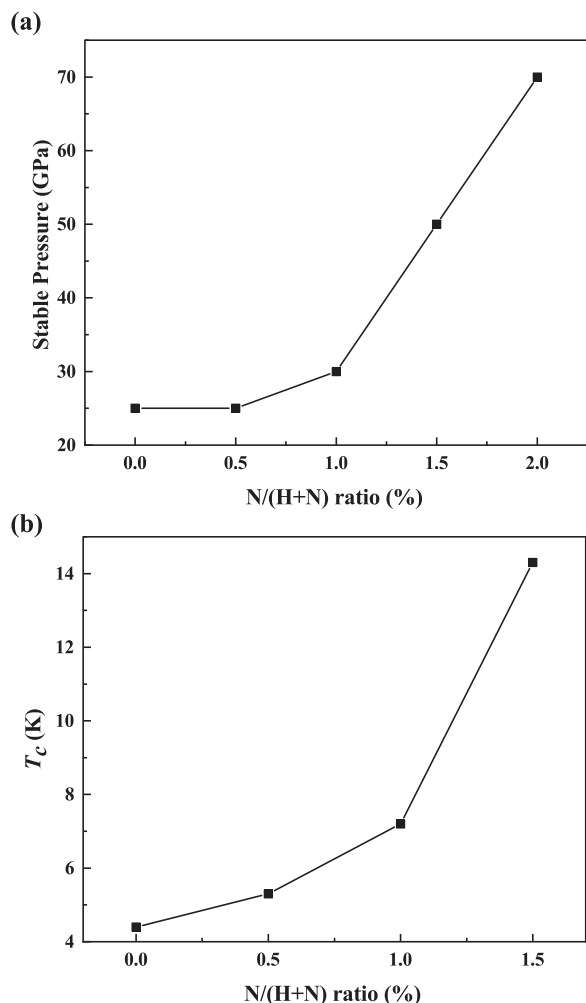
(a)

(b)

FIG. 4. (a) Dependence of minimum dynamically stable pressure on N-doping concentration. (b) Dependence of T_c on N-doping concentration at 50 GPa. The Coulomb pseudopotential uses $\mu^* = 0.10$.

with correction factors and a Coulomb pseudopotential[35] with $\mu^* = 0.10$ or 0.13.

III. RESULTS AND DISCUSSION

We performed a random structure search in the Lu–N–H system and constructed the ternary phase diagram (convex hull) at 1 GPa [Fig. 1(a)]. Some of the binary compounds were adopted from previous papers.[36–39] Notably, all predicted potential ternary compounds lie above the convex hull at 1 GPa. Thus, no ternary Lu–N–H compounds can remain thermodynamically stable at this pressure, which is consistent with the main results of Xie *et al.*[26] In addition, $P\bar{3}m1$-Lu$_2$H$_2$N was found with an enthalpy of ∼3 meV/atom above the convex hull. Detailed information about the structural parameters is listed in Table S1 (supplementary material). According to the inorganic crystal structure database, 20% of experimentally

synthesized materials are metastable.[40,41] Therefore, we calculated the x-ray diffraction (XRD) pattern for this metastable compound. Figure 1(b) shows a comparison of experimental and calculated XRD patterns. The calculated XRD pattern of $P\bar{3}m1$-Lu$_2$H$_2$N deviates clearly from the experimental one,[22] indicating that this compound does not occur in high-pressure experiments on N-doped lutetium hydride superconductors.

Next, we investigated the doping effect on N-doped LuH$_3$ using the supercell method. The cubic cell of Lu$_4$H$_m$N$_{12-m}$ was constructed by replacing hydrogen atoms with nitrogen atoms, for m = 8–11. For each concentration, we performed a geometry optimization on the configurations of various octahedral (O) and tetrahedral (T) sites [see Fig. 2(a)] and then calculated the total energy. Figures 2(b)–2(d) show the results for the formation enthalpy of Lu$_4$H$_m$N$_{12-m}$ at different pressures. At 1 GPa, only the formation enthalpy of Lu$_4$H$_{11}$N is negative (∼−24 meV/atom), indicating that this compound may be more stable than the others. A similar situation also occurs at 10 GPa (where the formation enthalpy is ∼−32 meV/atom for Lu$_4$H$_{11}$N). Thus, only Lu$_4$H$_{11}$N is thermodynamically encouraged to be formed below 10 GPa. At 50 GPa, Lu$_4$H$_{11}$N, Lu$_2$H$_5$N, Lu$_4$H$_9$N$_3$, and LuH$_2$N are thermodynamically encouraged to be formed. Thus, Lu$_4$H$_m$N$_{12-m}$ with low nitrogen doping is enthalpically favored at low pressure. The doping concentration of nitrogen increases with increasing pressure. In addition, when one nitrogen atom occupies a T site, the formation enthalpy of Lu$_4$H$_m$N$_{12-m}$ at 50 GPa is the lowest. Therefore, one nitrogen atom occupying a T site in Lu$_4$H$_m$N$_{12-m}$ is enthalpically preferred.

We then calculated the phonon spectra and superconducting properties of Lu$_4$H$_m$N$_{12-m}$. T_c values were estimated using the A-D-M equation with correction factors (Table S2, supplementary material). At 1 and 10 GPa, Lu$_4$H$_m$N$_{12-m}$ cannot dynamically stabilize, which may be due to the thermodynamical[42] and dynamical instability of the parent $Fm\bar{3}m$-LuH$_3$ [see Fig. S2(b), supplementary material]. At 50 GPa, only $R3m$-Lu$_2$H$_5$N can dynamically stabilize. The crystal structure, phonon spectrum, and EPC of $R3m$-Lu$_2$H$_5$N are illustrated in Fig. 3. $R3m$-Lu$_2$H$_5$N (Lu$_4$H$_{10}$N$_2$) can be regarded as $Fm\bar{3}m$-LuH$_3$ with two nitrogen atoms substituting its T and O sites, respectively. The calculated phonon spectrum and EPC show that the contributions of medium- and low-frequency phonons (13–25 THz) to the EPC are the highest (about 46% to total λ), whereas high-frequency phonons (45–55 THz) make hardly any contribution. Thus, the EPC of $R3m$-Lu$_2$H$_5$N is primarily contributed by medium- and low-frequency phonons. The calculated EPC parameter λ for $R3m$-Lu$_2$H$_5$N at 50 GPa in the harmonic approximation is 0.82. Using the calculated logarithmic average frequency ω_{log}, along with a Coulomb pseudopotential μ^* value of 0.1, the resultant T_c value is 27 K.

In the case of low nitrogen doping concentrations, we used the VCA method to investigate the pressure dependence of T_c in N-doped $Fm\bar{3}m$-LuH$_3$. Figure 4(a) shows the dependence of the minimum dynamically stable pressure on the N-doping concentration. We find that the minimum dynamically stable pressure of N-doped $Fm\bar{3}m$-LuH$_3$ increases from 25 to 70 GPa when the doping concentration increases from 0% to 2%. Thus, doping with N atoms will raise the dynamically stable pressure of LuH$_3$. Through a softening mechanism,[43] pressure can affect T_c by altering the electron–phonon constant λ. Therefore, we calculated the T_c of
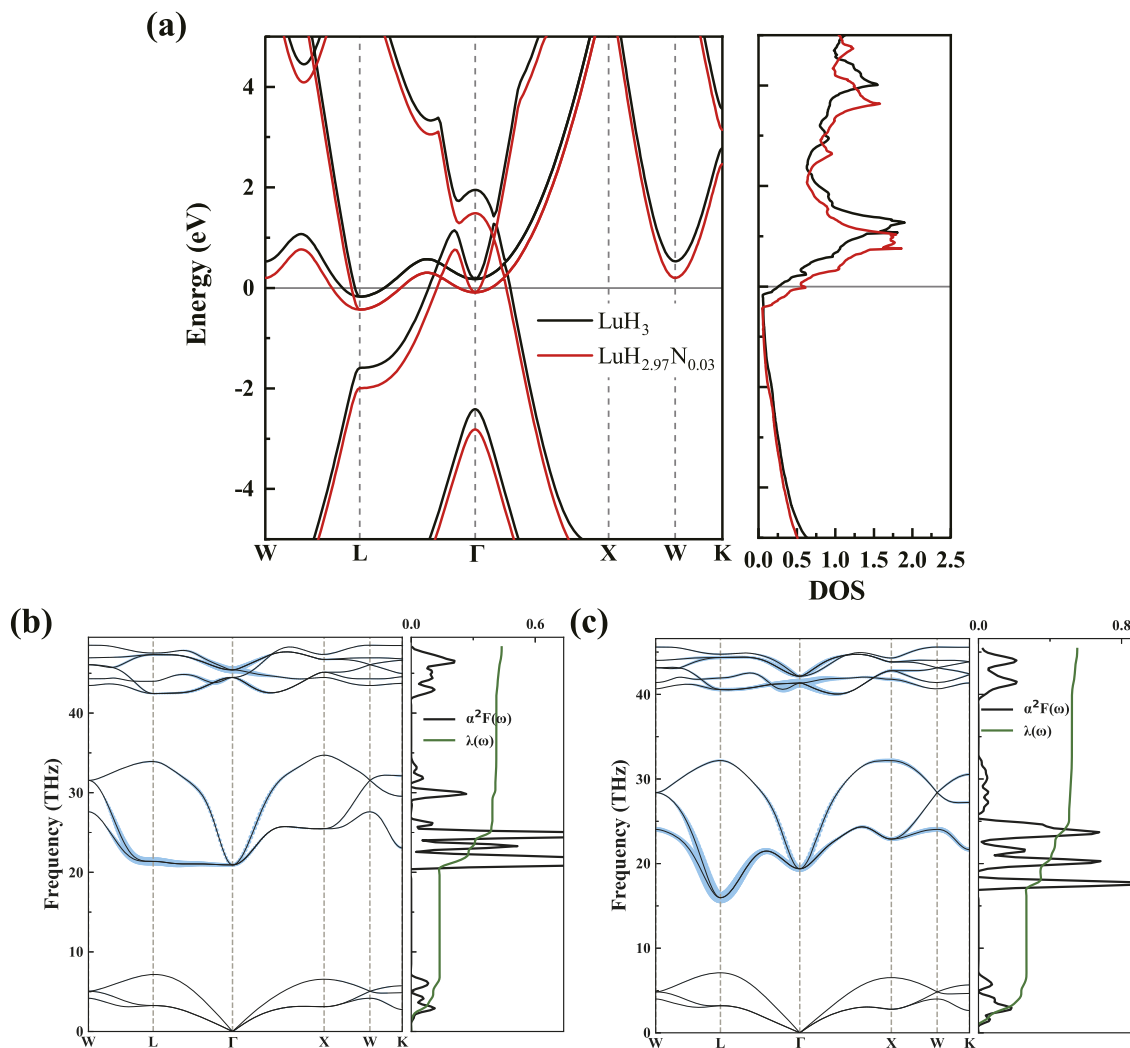
FIG. 5. (a) Electronic band structure and DOS (states eV^{-1} f.u.$^{-1}$) of LuH$_3$ (solid black curves) and LuH$_{2.97}$N$_{0.03}$ (solid red curves) at 50 GPa. The grey solid horizontal line indicates the Fermi energy. (b) and (c) Phonon spectra, Eliashberg phonon spectral function $\alpha^2 F(\omega)$, and electron–phonon integral λ for LuH$_3$ and LuH$_{2.97}$N$_{0.03}$, respectively, at 50 GPa. The magnitudes of the phonon linewidths are represented by the sizes of the blue circles.

N-doped LuH$_3$ with doping concentrations ranging from 0% to 1.5% at 50 GPa [see Fig. 4(b)] to investigate the effects of doping with nitrogen atoms on superconductivity. Our simulations show that the lowest T_c is 4 K for LuH$_3$ without doping. In addition, T_c increases with increasing N-doping concentration; thus, doping N atoms into LuH$_3$ will increase T_c. However, the highest T_c in this VCA calculation is 22 K, obtained with 1% N-doping at 30 GPa (see Table S2, supplementary material), which is much lower than room temperature. Notably, the anharmonicity correction to the atomic motions imposed by the large ionic quantum fluctuation will renormalize the phonon frequency in hydrogen-based superconductors. Therefore, the anharmonic effect may potentially decrease the dynamically stable pressure of N-doped LuH$_3$ and affect T_c, which requires further theoretical investigation in this system.

We calculated the band structure and density of states (DOS) of LuH$_3$ and LuH$_{2.97}$N$_{0.03}$ (1% N-doped) at 50 GPa [Fig. 5(a)]. The finite DOS at the Fermi level indicates the metallic nature of these structures. LuH$_3$ has a DOS $N(\epsilon_F)$ that reaches 0.269 states eV^{-1} f.u.$^{-1}$ at the Fermi level. Doping N atoms into LuH$_3$ will raise the Fermi level and cause the bands near the Γ point to fall on top of the Fermi level. Consequently, the Fermi level can be moved closer to the DOS peak, and $N(\epsilon_F)$ will then increase to 0.6 states eV^{-1} f.u.$^{-1}$ Therefore, doping by N atoms can significantly enhance the metallic characteristic of LuH$_3$ by moving the Fermi level closer to the DOS peak.

We then examined the phonon spectra and EPC of LuH$_3$ and LuH$_{2.97}$N$_{0.03}$ at 50 GPa [Figs. 5(b) and 5(c)]. In LuH$_3$, the electron–phonon constant λ is primarily contributed by the optical

branch (λ_{opt}), which accounts for ~69% of the total λ. Conversely, the acoustic branch (λ_{ac}) makes a much smaller contribution to λ, accounting for ~31% of the total λ. Doping by nitrogen atoms at 1% concentration increases λ_{ac} from 0.137 to 0.268, while λ_{opt} remains almost unchanged. Therefore, the increased T_c of N-doped LuH$_3$ can be attributed to the enhancement of λ_{ac}. Interestingly, the optical branch with a frequency of ~21 THz along the W–L–Γ direction in LuH$_3$ varies slightly with the wave vector $\boldsymbol{q}$ in the Brillouin zone. However, a significant softening of this phonon mode is observed after doping by nitrogen atoms [Fig. 5(c)]. When the pressure decreases to 25 GPa (Fig. S4, supplementary material), the imaginary phonon frequency occurs near the L point, which indicates that the optical branch softening induced by N doping is responsible for the reduced stability of LuH$_3$.

IV. CONCLUSIONS

We performed a first-principles study on the Lu–N–H system and found no stable ternary compounds at 1 GPa. We then analyzed N-doped $Fm\bar{3}m$-LuH$_3$ using supercell and VCA methods. The result of the supercell method indicates that $R3m$-Lu$_2$H$_5$N can be dynamically stable at 50 GPa, with a T_c of 27 K. The VCA results indicate that the highest T_c is 22 K, obtained with 1% N-doping at 30 GPa. In addition, doping with nitrogen atoms slightly increases the T_c of $Fm\bar{3}m$-LuH$_3$ by enhancing the EPC of acoustic phonons. However, this doping effect also leads to significant phonon softening and increases the dynamically stable pressure of LuH$_3$. Finally, within the pressure range investigated in our study, the highest T_c of N-doped $Fm\bar{3}m$-LuH$_3$ does not exceed 30 K, which is much lower than room temperature. Our theoretical calculations were performed using standard DFT parameters and assuming conventional superconductivity, and calculations considering more corrections, including strong electron correlations, spin–orbit coupling, the anharmonicity effect, and unconventional mechanisms of superconductivity are required in the future.

SUPPLEMENTARY MATERIAL

See the supplementary material for supplementary figures and tables.

ACKNOWLEDGMENTS

AUTHOR DECLARATIONS

Conflict of Interest

The authors have no conflicts to disclose.

Author Contributions

Zihao Huo: Conceptualization (equal); Data curation (equal); Formal analysis (equal); Writing – original draft (equal); Writing – review & editing (equal). **Defang Duan**: Conceptualization (lead); Formal analysis (lead); Funding acquisition (lead); Investigation (lead); Supervision (lead); Writing – review & editing (lead). **Tiancheng Ma**: Data curation (equal); Methodology (equal). **Zihan Zhang**: Conceptualization (supporting); Writing – review & editing (supporting). **Qiwen Jiang**: Writing – review & editing (supporting). **Decheng An**: Data curation (supporting). **Hao Song**: Conceptualization (supporting). **Fubo Tian**: Methodology (supporting). **Tian Cui**: Conceptualization (lead); Funding acquisition (lead); Methodology (equal); Supervision (equal); Writing – review & editing (equal).

DATA AVAILABILITY

The data that support the findings of this study are available within the article and its supplemental material and from the corresponding authors upon reasonable request.

REFERENCES

[1] C. J. Pickard, I. Errea, and M. I. Eremets, "Superconducting hydrides under pressure," Annu. Rev. Condens. Matter Phys. **11**, 57 (2020).

[2] D. Duan, Y. Liu, Y. Ma, Z. Shao, B. Liu, and T. Cui, "Structure and superconductivity of hydrides at high pressures," Natl. Sci. Rev. **4**, 121 (2017).

[3] X. Zhang, Y. Zhao, F. Li, and G. Yang, "Pressure-induced hydride superconductors above 200 K," Matter Radiat. Extremes **6**, 068201 (2021).

[4] H.-K. Mao, "Hydrogen and related matter in the pressure dimension," Matter Radiat. Extremes **7**, 063001 (2022).

[5] D. Duan, Y. Liu, F. Tian, D. Li, X. Huang, Z. Zhao, H. Yu, B. Liu, W. Tian, and T. Cui, "Pressure-induced metallization of dense (H$_2$S)$_2$H$_2$ with high-T_c superconductivity," Sci. Rep. **4**, 6968 (2014).

[6] A. P. Drozdov, M. I. Eremets, I. A. Troyan, V. Ksenofontov, and S. I. Shylin, "Conventional superconductivity at 203 kelvin at high pressures in the sulfur hydride system," Nature **525**, 73 (2015).

[7] M. Einaga, M. Sakata, T. Ishikawa, K. Shimizu, M. I. Eremets, A. P. Drozdov, I. A. Troyan, N. Hirao, and Y. Ohishi, "Crystal structure of the superconducting phase of sulfur hydride," Nat. Phys. **12**, 835 (2016).

[8] F. Peng, Y. Sun, C. J. Pickard, R. J. Needs, Q. Wu, and Y. Ma, "Hydrogen clathrate structures in rare earth hydrides at high pressures: Possible route to room-temperature superconductivity," Phys. Rev. Lett. **119**, 107001 (2017).

[9] H. Liu, I. I. Naumov, R. Hoffmann, N. W. Ashcroft, and R. J. Hemley, "Potential high-T_c superconducting lanthanum and yttrium hydrides at high pressure," Proc. Natl. Acad. Sci. U. S. A. **114**, 6990 (2017).

[10] A. P. Drozdov, P. P. Kong, V. S. Minkov, S. P. Besedin, M. A. Kuzovnikov, S. Mozaffari, L. Balicas, F. F. Balakirev, D. E. Graf, V. B. Prakapenka, E. Greenberg, D. A. Knyazev, M. Tkacz, and M. I. Eremets, "Superconductivity at 250 K in lanthanum hydride under high pressures," Nature **569**, 528 (2019).

[11] M. Somayazulu, M. Ahart, A. K. Mishra, Z. M. Geballe, M. Baldini, Y. Meng, V. V. Struzhkin, and R. J. Hemley, "Evidence for superconductivity above 260 K in lanthanum superhydride at megabar pressures," Phys. Rev. Lett. **122**, 027001 (2019).

[12] X. Li, X. Huang, D. Duan, C. J. Pickard, D. Zhou, H. Xie, Q. Zhuang, Y. Huang, Q. Zhou, B. Liu, and T. Cui, "Polyhydride CeH$_9$ with an atomic-like hydrogen clathrate structure," Nat. Commun. **10**, 3461 (2019).

[13] F. Hong, L. Yang, P. Shan, P. Yang, Z. Liu, J. Sun, Y. Yin, X. Yu, J. Cheng, and Z. Zhao, "Superconductivity of lanthanum superhydride investigated using the standard four-probe configuration under high pressures," Chin. Phys. Lett. **37**, 107401 (2020).

[14] H. Xie, Y. Yao, X. Feng, D. Duan, H. Song, Z. Zhang, S. Jiang, S. A. T. Redfern, V. Z. Kresin, C. J. Pickard, and T. Cui, "Hydrogen pentagraphenelike structure

stabilized by hafnium: A high-temperature conventional superconductor," Phys. Rev. Lett. **125**, 217001 (2020).

[15] P. Kong, V. S. Minkov, M. A. Kuzovnikov, A. P. Drozdov, S. P. Besedin, S. Mozaffari, L. Balicas, F. F. Balakirev, V. B. Prakapenka, S. Chariton, D. A. Knyazev, E. Greenberg, and M. I. Eremets, "Superconductivity up to 243 K in the yttrium-hydrogen system under high pressure," Nat. Commun. **12**, 5075 (2021).

[16] Z. Zhang, T. Cui, M. J. Hutcheon, A. M. Shipley, H. Song, M. Du, V. Z. Kresin, D. Duan, C. J. Pickard, and Y. Yao, "Design principles for high-temperature superconductors with a hydrogen-based alloy backbone at moderate pressure," Phys. Rev. Lett. **128**, 047001 (2022).

[17] L. Ma, K. Wang, Y. Xie, X. Yang, Y. Wang, M. Zhou, H. Liu, X. Yu, Y. Zhao, H. Wang, G. Liu, and Y. Ma, "High-temperature superconducting phase in clathrate calcium hydride CaH_6 up to 215 K at a pressure of 172 GPa," Phys. Rev. Lett. **128**, 167001 (2022).

[18] M. Du, H. Song, Z. Zhang, D. Duan, and T. Cui, "Room-temperature superconductivity in Yb/Lu substituted clathrate hexahydrides under moderate pressure," Research **2022**, 9784309.

[19] H. Song, Z. Zhang, T. Cui, C. J. Pickard, V. Z. Kresin, and D. Duan, "High T_c superconductivity in heavy rare earth hydrides," Chin. Phys. Lett. **38**, 107401 (2021).

[20] M. Shao, S. Chen, W. Chen, K. Zhang, X. Huang, and T. Cui, "Superconducting ScH_3 and LuH_3 at megabar pressures," Inorg. Chem. **60**, 15330 (2021).

[21] Z. Li, X. He, C. Zhang, K. Lu, B. Bin, J. Zhang, S. Zhang, J. Zhao, L. Shi, S. Feng, X. Wang, Y. Peng, R. Yu, L. Wang, Y. Li, J. Bass, V. Prakapenka, S. Chariton, H. Liu, and C. Jin, "Superconductivity above 70 K experimentally discovered in lutetium polyhydride," Sci. China Phys. Mech **66**, 267411 (2023).

[22] N. Dasenbrock-Gammon, E. Snider, R. McBride, H. Pasan, D. Durkee, N. Khalvashi-Sutter, S. Munasinghe, S. E. Dissanayake, K. V. Lawler, A. Salamat, and R. P. Dias, "Evidence of near-ambient superconductivity in a N-doped lutetium hydride," Nature **615**, 244 (2023).

[23] P. Shan, N. Wang, X. Zheng, Q. Qiu, Y. Peng, and J. Cheng, "Pressure-induced color change in the lutetium dihydride LuH_2," Chin. Phys. Lett. **40**, 046101 (2023).

[24] X. Ming, Y.-J. Zhang, X. Zhu, Q. Li, C. He, Y. Liu, B. Zheng, H. Yang, and H.-H. Wen, "Absence of near-ambient superconductivity in $LuH_{2\pm x}N_y$," arXiv:2303.08759 (2023).

[25] M. Liu, X. Liu, J. Li, J. Liu, Y. Sun, X.-Q. Chen, and P. Liu, "On parent structures of near-ambient nitrogen-doped lutetium hydride superconductor," arXiv:2303.06554 (2023).

[26] F. Xie, T. Lu, Z. Yu, Y. Wang, Z. Wang, S. Meng, and M. Liu, "Lu-H-N phase diagram from first-principles calculations," Chin. Phys. Lett **40**, 057401 (2023) .

[27] C. J. Pickard and R. J. Needs, "*Ab initio* random structure searching," J. Phys.: Condens. Matter **23**, 053201 (2011).

[28] M. D. Segall, P. J. D. Lindan, M. J. Probert, C. J. Pickard, P. J. Hasnip, S. J. Clark, and M. C. Payne, "First-principles simulation: Ideas, illustrations and the CASTEP code," J. Phys.: Condens. Matter **14**, 2717 (2002).

[29] P. E. Blöchl, "Projector augmented-wave method," Phys. Rev. B **50**, 17953 (1994).

[30] G. Kresse and D. Joubert, "From ultrasoft pseudopotentials to the projector augmented-wave method," Phys. Rev. B **59**, 1758 (1999).

[31] G. Kresse and J. Furthmüller, "Efficiency of ab-initio total energy calculations for metals and semiconductors using a plane-wave basis set," Comput. Mater. Sci. **6**, 15 (1996).

[32] J. P. Perdew, K. Burke, and M. Ernzerhof, "Generalized gradient approximation made simple," Phys. Rev. Lett. **77**, 3865 (1996).

[33] P. Giannozzi, S. Baroni, N. Bonini, M. Calandra, R. Car, C. Cavazzoni, D. Ceresoli, G. L. Chiarotti, M. Cococcioni, I. Dabo *et al.*, "QUANTUM ESPRESSO: A modular and open-source software project for quantum simulations of materials," J. Phys.: Condens. Matter **21**, 395502 (2009).

[34] P. B. Allen and R. C. Dynes, "Transition temperature of strong-coupled superconductors reanalyzed," Phys. Rev. B **12**, 905 (1975).

[35] P. Morel and P. W. Anderson, "Calculation of the superconducting state parameters with retarded electron-phonon interaction," Phys. Rev. **125**, 1263 (1962).

[36] J. E. Bonnet and J. N. Daou, "Rare-earth dihydride compounds: Lattice thermal expansion and investigation of the thermal dissociation," J. Appl. Phys. **48**, 964 (1977).

[37] M. Mansmann and W. E. Wallace, "The structure of HoD_3," J. Phys. France **25**, 454 (1964).

[38] W. Klemm and G. Winkelmann, "Zur kenntnis der nitride der seltenen erdmetalle," Z. Anorg. Allg. Chem. **288**, 87 (1956).

[39] R. Boese, N. Niederprüm, D. Bläser, A. Maulitz, M. Y. Antipin, and P. R. Mallinson, "Single-crystal structure and electron density distribution of ammonia at 160 K on the basis of X-ray diffraction data," J. Phys. Chem. B **101**, 5794 (1997).

[40] Y. Hinuma, T. Hatakeyama, Y. Kumagai, L. A. Burton, H. Sato, Y. Muraba, S. Iimura, H. Hiramatsu, I. Tanaka, H. Hosono, and F. Oba, "Discovery of earth-abundant nitride semiconductors by computational screening and high-pressure synthesis," Nat. Commun. **7**, 11962 (2016).

[41] Y. Wu, P. Lazic, G. Hautier, K. Persson, and G. Ceder, "First principles high throughput screening of oxynitrides for water-splitting photocatalysts," Energy Environ. Sci. **6**, 157 (2013).

[42] T. Palasyuk and M. Tkacz, "Pressure-induced structural phase transition in rare-earth trihydrides. Part I. (GdH_3, HoH_3, LuH_3)," Solid State Commun. **133**, 481 (2005).

[43] W. L. McMillan, "Transition temperature of strong-coupled superconductors," Phys. Rev. **167**, 331 (1968).